



Magnetic field assisted laser cladding to prepare crack-free Fe-Cr-Mo-C-Y-B amorphous coating

Journal:	<i>Philosophical Magazine & Philosophical Magazine Letters</i>
Manuscript ID	TPHL-2019-0112
Journal Selection:	Philosophical Magazine Letters
Date Submitted by the Author:	11-Nov-2019
Complete List of Authors:	Zhang, Qi; Shanghai University of Engineering Science, School of Materials Engineering zhang, peilei; Shanghai University of Engineering Science yan, hua; Shanghai University of Engineering Science Yu, Zhishui; Shanghai University of Engineering Science Wu, Di; Shanghai University of Engineering Science, School of Materials Engineering Shi, Haichuan; Shanghai University of Engineering Science, School of Materials Engineering Li, Shaowei; Shanghai University of Engineering Science, School of Materials Engineering
Keywords:	amorphous alloys, laser surface engineering, coatings, metallic glasses
Keywords (user supplied):	Crack-free, Laser cladding

SCHOLARONE™
Manuscripts

Magnetic field assisted laser cladding to prepare crack-free Fe-Cr-Mo-C-Y-B amorphous coating

Qi Zhang^{1,2}, Peilei Zhang^{1,2,1*}, Hua Yan^{1,2}, Zhishui Yu^{1,2}, Di Wu^{1,2}, Haichuan Shi^{1,2}, Shaowei Li

^{1,2}

1. School of Materials Engineering, Shanghai University of Engineering Science, Shanghai

201620, China

2. Shanghai Collaborative Innovation Center of Laser Advanced Manufacturing Technology,

Shanghai 201620, China

Abstract

The physical properties of Q235 steel and Fe-based amorphous material are quite different. The laser cladding method can produce defects such as cracks on the surface of amorphous coating. In this paper, the Fe-based amorphous coating is prepared by the method of magnetic field assisted laser cladding. The uniformity of the element distribution in the coating is increased by the stirring of the magnetic field, which increases the plastic toughness of the coating. And the crack-free Fe-Cr-Mo-C-Y-B amorphous coating was successfully prepared on the surface of Q235. The mechanical behavior of the indentation points after nanoindentation was observed by TEM.

Keywords: Crack-free; Coating; Laser cladding; Surface alloying; Amorphous materials;

1. Introduction

Amorphous alloy, also known as metallic glass, has the advantages of metal and glass [1].

However, amorphous alloys have size limitations that make amorphous alloys difficult to become

* Corresponding author at: Room 3109, School of Materials Engineering, 333 Long Teng Rd. Songjiang Campus of Shanghai University of Engineering Science, Shanghai, 201620, China. Tel: +86 21 67761412; Fax: +86 21 67791377. Email addresses: peilei@sues.edu.cn (Peilei Zhang).

1
2
3
4 a new generation of structural materials [2-3]. The preparation method of the amorphous coating
5
6 mainly includes laser cladding and thermal spray-based techniques. The coating prepared by laser
7
8 cladding has good metallurgical bonding property with the substrate, and the surface properties of
9
10 the matrix alloy are remarkably improved [4]. Previously Aghasibeig et al. [5] investigated the
11
12 laser cladding experiments with Fe-Cr-Mn-Si-Mo-C alloy on AISI 1018 steel substrates using a
13
14 diode laser.
15
16
17
18

19
20 However, these techniques have their own drawbacks like other technologies. Owing to the
21
22 faster cooling rate, the residual stress inside the coating is larger during solidification, especially
23
24 the solidification crack and the fragile precipitation phase of the network distribution [6]. These
25
26 shortcomings greatly limit the industrial application of laser cladding technology.
27
28
29

30
31 In the laser cladding process, gradient heating or addition of toughening elements is usually
32
33 used to control the formation of cracks [7]. However, these methods do not completely and
34
35 generally eliminate cracks. Recently, Lu et al. [8] have successfully prevented the propagation of
36
37 cracks during the laser cladding of Fe-Cr-C-B-Mo amorphous coating by using a triple laser
38
39 scanning strategy. To circumvent some of these problems, in this paper, we successfully obtained
40
41 a crack-free amorphous coating by adding a longitudinal alternating magnetic field. The agitation
42
43 of the liquid coating by the alternating magnetic field reduces the internal stress generated by the
44
45 coating during solidification.
46
47
48
49
50

51 **2. Experimental**

52
53 Fe-based amorphous coating was prepared by laser cladding on the surface of Q235. Table 1
54
55 showed the as-received chemical composition of the powder. A 5 Kw high power continuous
56
57 wave fiber optic IPG laser was employed for laser processing of glass metal coating on steel. The
58
59
60

laser wavelength was 1070nm, and the spot was configured to provide circular spot with a radius of 0.3mm. The longitudinal alternating magnetic field is generated by a toroidal magnetic coil.

Table 1 Chemical composition of the amorphous alloy powder (wt.%).

Element	Cr	Mo	C	Y	B	Fe
wt.%	14.32-15.02	25.10-26.2	3.24-3.75	3.10-3.60	1.10-1.42	Bal.

3. Results and discussion

The XRD patterns produced by different cladding layers at different magnetic field strengths are shown in Fig. 1. Obviously, the change in magnetic field strength has no significant effect on the composition of the phase in the coating. The phase composition of different coatings is mainly composed with $M_{23}C_6$ (M=Fe,Cr,Mo), γ -(Fe,Cr,Mo) and some bcc-Fe. But it can be seen easy that as the speed increases crystalline peaks were decreased, the wider diffraction peaks appear at $2\theta=45^\circ$ and the peaks intensity which representing the content of γ -Fe and bcc-Fe was decreasing. Fig. 2(b) shows the XRD peak near 45° . The increase in the strength of the magnetic field causes the peak of the crystalline phase in the coating to decrease, demonstrating an increase in the amorphous phase content of the coating.

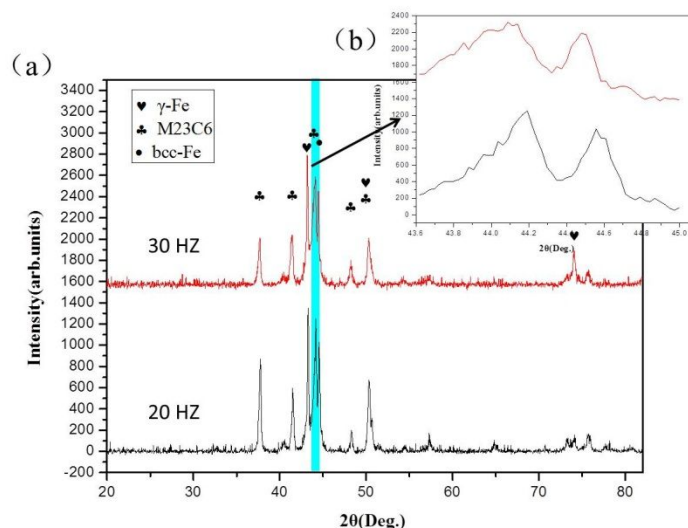


Fig 2 XRD patterns of the coating at different magnetic field strength

Fig. 2 shows the macroscopic morphology of the laser-clad iron-based amorphous coating at different magnetic field frequencies. The cracks, which generated due to the rapid solidification rate resulting in the residual stress not being completely released (Fig. 2a). After the addition of the longitudinal alternating magnetic field, the residual stress before solidification is released due to the stirring action of the longitudinal alternating magnetic field to change the coating morphology and reduce the crack generation (Fig. 2b, c). And as the frequency of the magnetic field increases, the crack in the coating tends to disappear. During the solidification of the metal, the dendritic structure can freely flow in the initial molten pool having a lower solid fraction. However, as the dendrites that grow and solidify form a dendritic network, only a small part of the liquid phase can flow and is affected by the dendritic network. A strong agitation is applied to the molten metal by introducing a magnetic field. Between the solid phase particles which are precipitated first, strong collision and friction between the solid phase and the liquid phase cause the temperature gradient of the solid phase particles to be uniform.

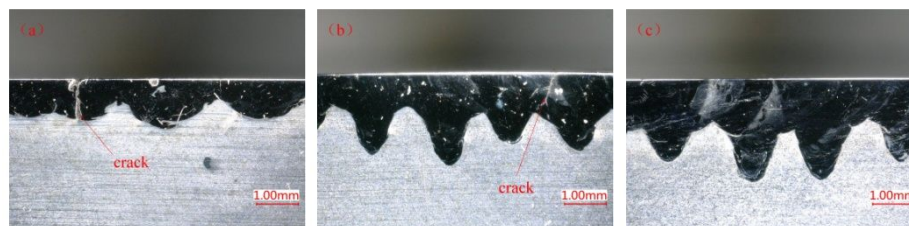


Fig.3 Laminated coating macroscopic morphology (a) 10HZ (b) 20HZ (c) 30HZ

Mapping scanning results of the coating is shown in Fig.3(d,e,f). It can be seen that although the element distribution is relatively uniform under the action of the magnetic field, Mo mainly concentrated in the white region. Combined with XRD, the white primary phase in the coating is γ -(Fe,Cr,Mo). The gray area is mainly a mixed area of $M_{23}C_6$ and an amorphous phase. The edge region mainly contains bcc-Fe. In the amorphous coating of Fe-Cr-Mo-C-Y series $(Fe,Cr)_{23}C_6$ is very common to be calibrated. However, the appearance of Mo in this experiment proves that $M_{23}C_6$ is not just a simple ternary mixture by Fe,Cr,C. The presence of a small amount of Mo results in the presence of $M_{23}C_6$ as $(Cr, Fe)_{20}(Cr, Fe, Mo)_3C_6$. $M_{23}C_6$ has a small amount of Mo dissolves in the second sublattice compared to FE [10].

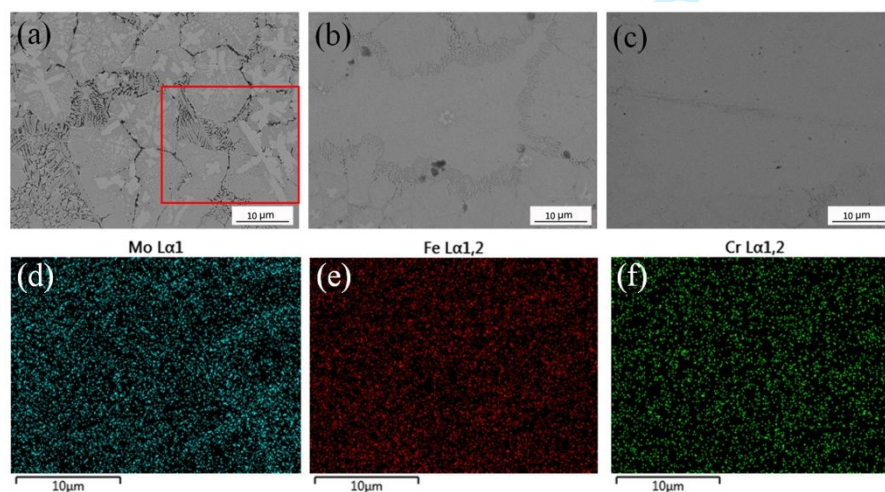


Fig. 3 Morphology of the coating (a-c) 10 20 30(HZ) (d-f) Mapping scanning

1
2
3
4
5
6
7 The morphology of the coating at different magnetic field frequencies is shown in the Fig. 3.
8
9 In the solidification process of the amorphous coating, $(\text{Fe,Cr,Mo})_{23}\text{C}_6$ and $\gamma\text{-(Fe,Cr,Mo)}$ is mainly
10 produced, and Fe, Cr, and Mo can be substituted with each other. However, when no magnetic
11 field is introduced, Mo is purely in $\gamma\text{-(Fe,Cr,Mo)}$. The addition of a magnetic field creates a strong
12 agitation in the molten coating to promote the homogenization of the distribution of Mo. Fig. 3(c)
13 shows that when the magnetic field frequency is 20 Hz. It can be seen that as the magnetic field
14 strength increases, the volume of the $\gamma\text{-(Fe,Cr,Mo)}$ phase in the coating decreases. And the shape
15 tends to be more spherical. That is because the molten metal will generate a volume force under
16 the stirring of the magnetic field, and this volume force will cause the macroscopic flow of the
17 metal melt and become the kinetic condition of the primary crystal nucleation. In the partial area
18 of Figure 3, and it can be seen that fine dendrites appear in the boundary area instead of the
19 original bcc-fe. The dendrites are closely connected to each other, which reduces the tendency of
20 cracks at the boundary and increases the toughness of the coating. When the frequency of the
21 magnetic field strength is increased to 30HZ, a large volume of amorphous gray phase can be seen
22 in the coating, it can be seen in Fig. 3(d). This means that the homogenization of the elements
23 promotes an increase in the amorphous phase content of the coating under agitation of the
24 magnetic field.
25
26
27
28
29
30
31
32
33
34
35
36
37
38
39
40
41
42
43
44
45
46
47
48
49
50

51 In order to further test the mechanical properties of the coating, the mixed area of M_{23}C_6 and
52 amorphous phase in the coating was tested by nanoindentation. And the indentation point was
53 sampled by FIB method and the TEM test results were shown in the Fig. 4. The effect of the
54 external force does not cause the fracture of the relatively fragile grain boundary, which indicates
55
56
57
58
59
60

1
2
3
4 that the addition of the magnetic field makes the element homogenization in the coating enhance
5
6 the plastic toughness of the grain boundary (Fig. 4b). Although no cracks appeared near the
7
8 nanoindentation point, the surrounding grains produced plastic deformation and dislocation
9
10 accumulation during the nanoindentation experiment. Amorphous and nanocrystalline generally
11
12 occur together when laser cladding is used to prepare an amorphous coating as shown in Fig. 4(b).
13
14 The TEM high magnification is shown in Fig. 4(c) can clearly see that the directions on both sides
15
16 of the crystal lattice are inconsistent, but present two parts symmetrical about the grain boundary.
17
18 This structure is a typical coherent twin boundary.
19
20
21
22
23
24
25
26
27
28
29
30
31
32
33
34
35
36
37
38
39
40
41
42
43
44
45
46
47
48
49
50
51
52
53
54
55
56
57
58
59
60

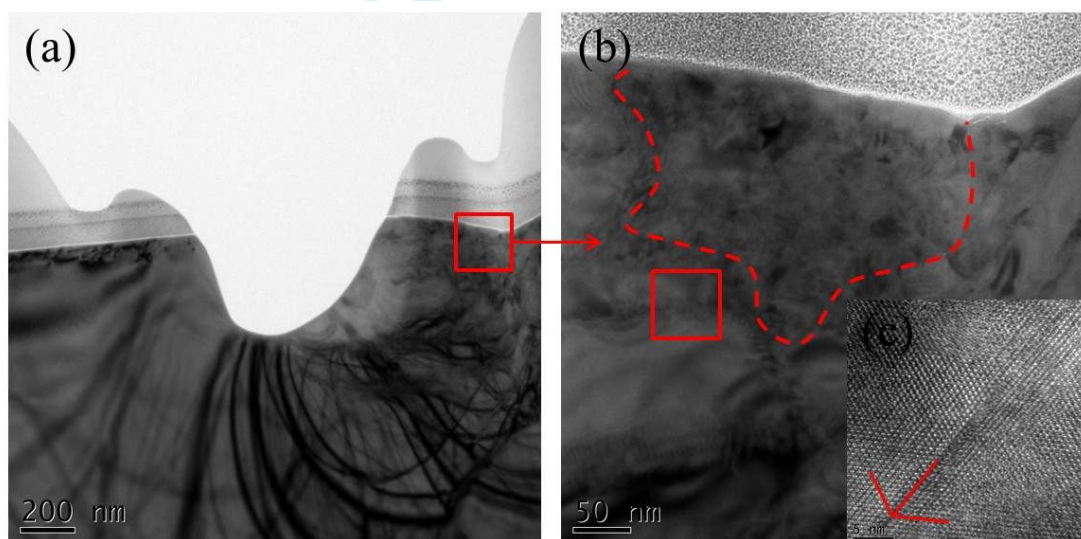


Fig. 4 (a,b) TEM images of nanoindentation point (c) HRTEM images

4. Conclusions

The crack-free Fe-Cr-Mo-C-Y-B amorphous coating was successfully prepared by the method of longitudinal alternating magnetic field assisted laser cladding. The introduction of the magnetic field produces a stirring effect on the molten coating, which not only makes the distribution of elements in the coating more uniform, but also increases the plastic toughness of

1
2
3
4 the coating, and the amorphous content also increases. Transmission electron microscopy analysis
5
6 of the nanoindentation points showed that although there were many dislocations and vacancies
7
8 near the indentation point, no crack appeared to prove that the coating had high plastic toughness,
9
10 and the presence of amorphous was found.
11
12
13
14
15
16
17
18
19

20 **Acknowledgements**

21
22 This research was supported by Foundation of Natural Science Foundation of China (51605276,
23
24 51905333), Shanghai Sailing Program (19YF1418100), Shanghai Science and Technology
25
26 Committee Innovation Grant (17JC1400600, 17JC1400601), Karamay Science and Technology
27
28 Major Project (2018ZD002B), Aid for Xinjiang Science and Technology Project (2019E0235),
29
30 Shanghai local colleges and universities capacity building special plan project (19030501300).
31
32
33
34
35
36
37
38
39
40
41
42
43
44

45 **References**

- 46
47
48 [1] B. Huang, Y. Yang, A. Wang, Q. Wang, C. Liu, Saturated magnetization and glass forming
49
50 ability of soft magnetic Fe-based metallic glasses, *Intermetallics*. 84 (2017) 74–81.
51
52
53 [2] M. Jafary-Zadeh, G. Praveen Kumar, P.S. Branicio, M. Seifi, J.J. Lewandowski, F. Cui, A
54
55 critical review on metallic glasses as structural materials for cardiovascular stent applications,
56
57 *J. Funct. Biomater.* (2018) 9.
58
59
60

- 1
2
3
4 [3] S. Pauly, L. Löber, R. Petters, M. Stoica, S. Scudino, U. Kühn, J. Eckert, Processing metallic
5
6 glasses by selective laser melting, *Mater.* 16 (2013) 37–41.
7
8
9 [4] C.Y. Yang, X. Cheng, H.B. Tang, X.J. Tian, D. Liu, Influence of microstructures and wear
10
11 behaviors of the microalloyed coatings on TC11 alloy surface using laser cladding technique,
12
13 *Surf. Coat.* 337 (2018) 97–103.
14
15
16 [5] Z. Zhang, T. Yu, R. Kovacevic, Erosion and corrosion resistance of laser cladding 420
17
18 stainless steel reinforced with VC, *Appl Surf Sci.* 410 (2017) 225–240.
19
20
21 [6] Xie S , Li R , Yuan T , et al. Laser cladding assisted by friction stir processing for preparation
22
23 of deformed crack-free Ni-Cr-Fe coating with nanostructure, *Optics & Laser Technology.*
24
25 (2017)
26
27
28 [7] C Zhikun, L Ming, Z Dechang, Research on formation causes and elimination methods of the
29
30 laser cladding cracks, *Laser J.* 30 (2009) 55–57.
31
32
33 [8] L Yunzhuo, H Guokun, W Yongzhe, L Hongge, Crack-free Fe-based amorphous coating
34
35 synthesized by laser cladding, *Mater Lett.* 210 (2018) 46-50.
36
37
38 [9] R Hirayama, K Fujisaki, T Yamada. Dual In-Mold Electromagnetic Stirring in Continuous
39
40 Casting, *IEEE Transactions on Magnetics.* 40(2004) 2095-2097.
41
42
43 [10] M. Hillert, C.Qiu, A reassessment of the Fe-Cr-Mo-C system, *Journal of Phase Equilibria.* 13
44
45 (1992) 512-521. <https://doi.org/10.1007/bf02665764>.
46
47
48
49
50
51
52
53
54
55
56
57
58
59
60

- 1
 - 2
 - 3
 - 4
 - 5
 - 6
 - 7
 - 8
 - 9
 - 10
 - 11
 - 12
 - 13
 - 14
 - 15
 - 16
 - 17
 - 18
 - 19
 - 20
 - 21
 - 22
 - 23
 - 24
 - 25
 - 26
 - 27
 - 28
 - 29
 - 30
 - 31
 - 32
 - 33
 - 34
 - 35
 - 36
 - 37
 - 38
 - 39
 - 40
 - 41
 - 42
 - 43
 - 44
 - 45
 - 46
 - 47
 - 48
 - 49
 - 50
 - 51
 - 52
 - 53
 - 54
 - 55
 - 56
 - 57
 - 58
 - 59
 - 60
1. The introduction of a magnetic field reduces the tendency to crack during laser cladding of an iron-based amorphous process.
 2. A new mode of mixing amorphous and crystalline phases was found in iron-based amorphous coatings.
 3. The addition of a magnetic field results in a crack-free coating and increases the amorphous content.
 4. The mechanical behavior at the nanoindentation point was observed by TEM.

For Peer Review Only

Table 1 Chemical composition of the amorphous alloy powder (wt.%).

Element	Cr	Mo	C	Y	B	Fe
wt.%	14.32-15.0	25.10-26.2	3.24-3.75	3.10-3.60	1.10-1.42	Bal.

For Peer Review Only